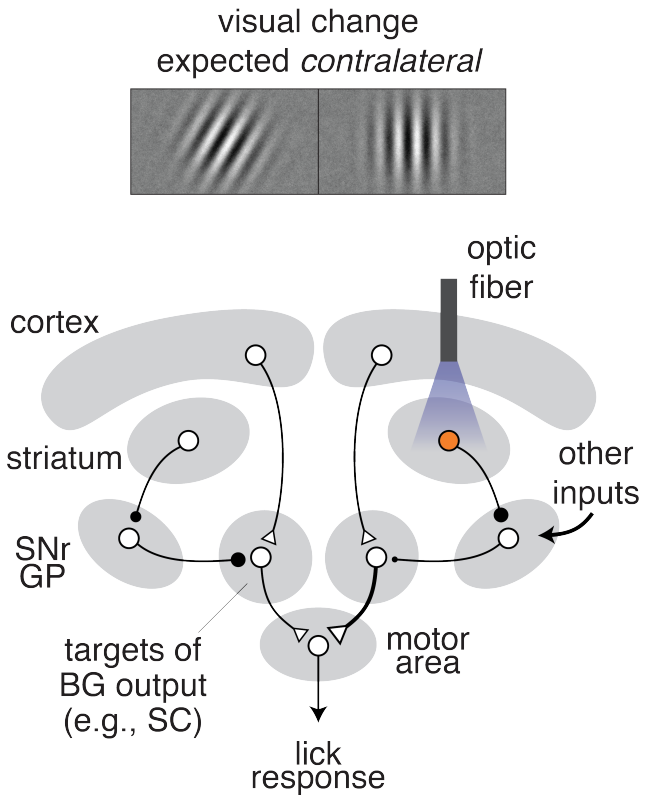

Figure S1: Schematic model of circuits affected by activation of striatal dMSNs (related to Figure 2)

Schematic model illustrating a simple explanation for the results of dMSN activation based on the lateralized organization of outputs from the basal ganglia. Black circles indicate inhibitory synapses and white triangles indicate excitatory synapses. Activation of dMSNs would tend to facilitate licks that were evoked mostly by stimulus events expected in the contralateral visual field, because the sensory-motor structures targeted by the activation in our experiments also receive predominantly uncrossed cortical inputs and are presumed to receive different levels of inhibition (indicated by the differently sized black circles) depending on the context. There are several good candidates for the “other inputs” to BG output nuclei that could give rise to the asymmetric disinhibition on these sensory-motor structures – for example, the hyperdirect pathway. A similar scheme might also be applied to iMSNs with different inhibition to basal ganglia output targets.

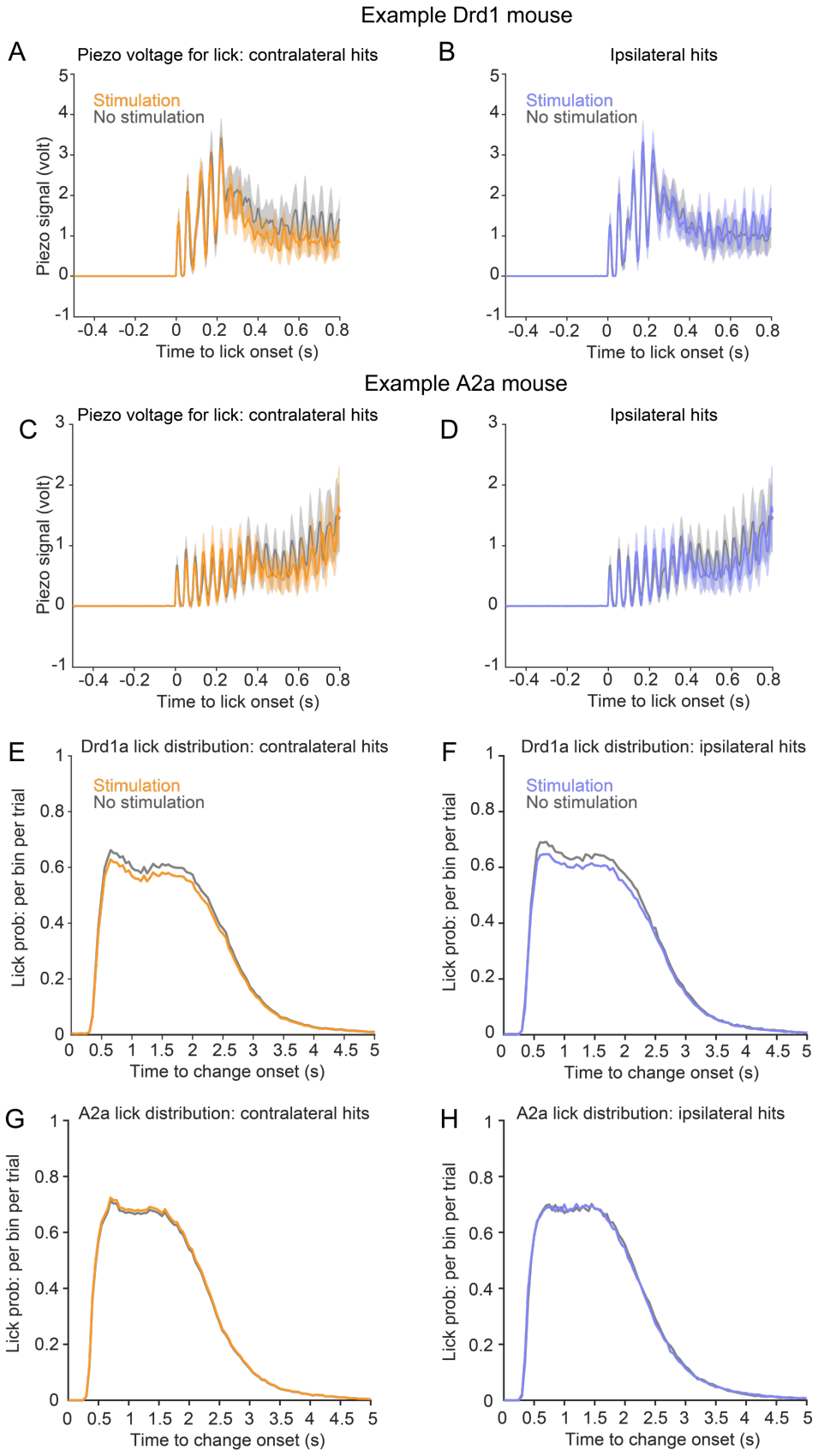
Example Drd1 mouse
A
Piezo voltage for lick: contralateral hits
Stimulation
No stimulation
Piezo signal (volt)
Time to lick onset (s)
B
Ipsilateral hits
Stimulation
No stimulation
Time to lick onset (s)
Example A2a mouse
C
Piezo voltage for lick: contralateral hits
Piezo signal (volt)
Time to lick onset (s)
D
Ipsilateral hits
Time to lick onset (s)
E
Drd1a lick distribution: contralateral hits
Stimulation
No stimulation
Lick prob: per bin per trial
Time to change onset (s)
F
Drd1a lick distribution: ipsilateral hits
Stimulation
No stimulation
Lick prob: per bin per trial
Time to change onset (s)
G
A2a lick distribution: contralateral hits
Lick prob: per bin per trial
Time to change onset (s)
H
A2a lick distribution: ipsilateral hits
Lick prob: per bin per trial
Time to change onset (s)

Figure S2: Effects of striatal stimulation on the vigor of lick responses (related to Figure 5)

(A) Piezo voltage amplitude evoked by licking from an example Drd1a mice in hit trials with orientation change in the contralateral hemifield, with (orange) and without (gray) optogenetic stimulation. Time zero is defined as reaction time. Thick lines represent mean and shading indicates 95% CI of mean. (B) Piezo voltage amplitude evoked by licking from the same example Drd1a mice in hit trials with orientation change in the ipsilateral hemifield, with (blue) and without (gray) optogenetic stimulation. (C-D) Piezo voltage amplitude evoked by licking from an example A2a mice in hit trials with orientation change in the contralateral and ipsilateral hemifield, with and without stimulation. In all cases (A-D) piezo voltage traces with and without stimulation overlapped over their entire time courses.

(E) Distribution of Drd1a mice population (n=10) lick probability in all hit trials with orientation change in the contralateral hemifield, with (orange) and without (gray) optogenetic stimulation. Bin width: 50-ms, thick lines represent population mean and shading indicates 95% CI. (F) Distribution of Drd1a population lick probability in all ipsilateral hit trials with and without stimulation. (G-H) Distribution of A2a population (n=12) lick probability in all hit trials with orientation change in the contralateral (G) and ipsilateral hemifield, with and without stimulation. Activation of MSNs did not change the frequency of licking.

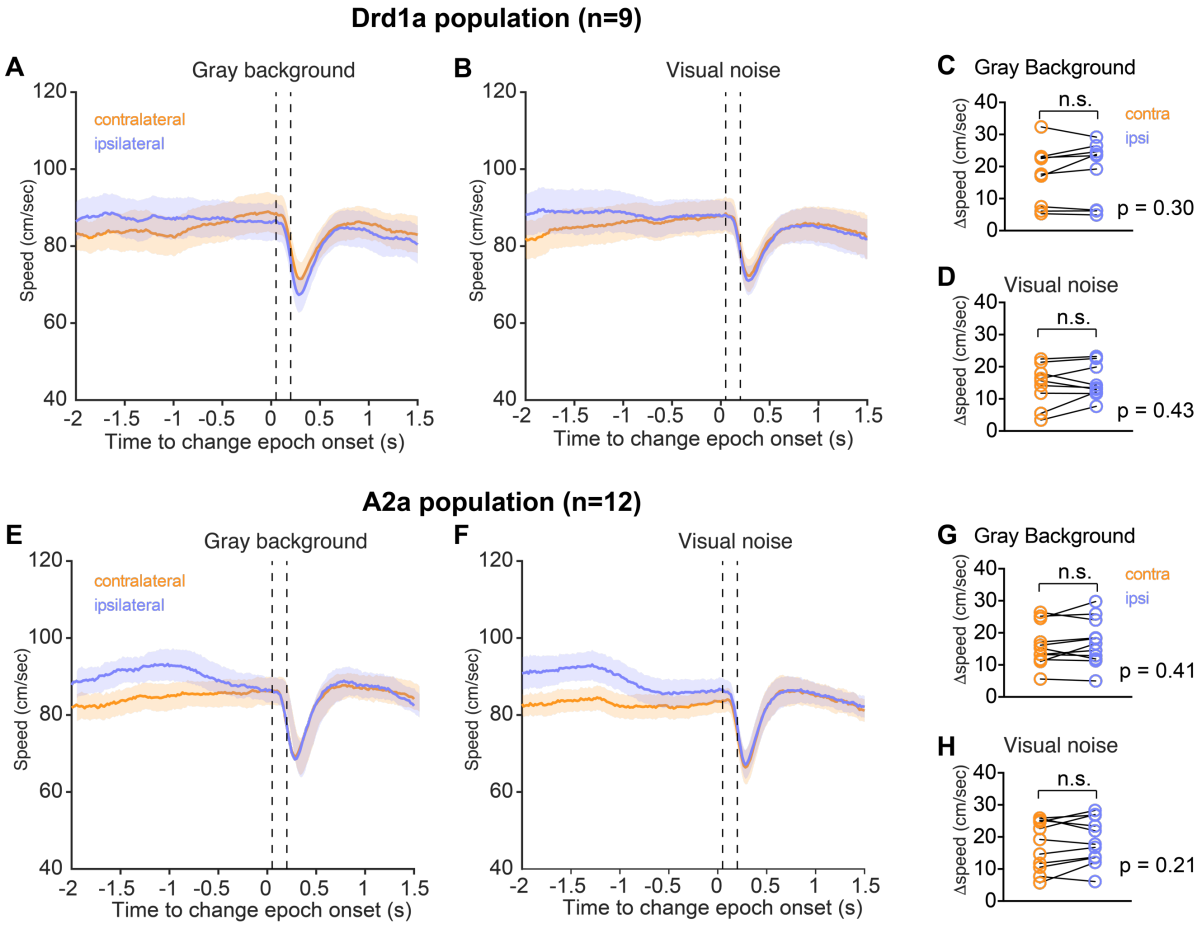

Figure S3: Effects of striatal stimulation on running speed (related to Figure 5)

(A) Population running speed of Drd1a mice when stimulation was applied during 'sequence-arrested control' trials with only the gray background presented; stimulation in these trials did not evoke licking and thus avoided the confound that mice tend to stop running when they lick. The two vertical dashed lines indicate the onset and offset of optic stimulation. Thick lines represent population mean and shading indicates SEM. (B) Population running speed of Drd1a mice with stimulation during trials only visual noise was presented. (C-D) The amplitude of direct pathway stimulation induced transient running speed reduction did not show significant difference between contralateral and ipsilateral blocks in either trial types. (E-F) population running speed of A2a mice when stimulation was applied during gray background and visual noise trials. (G-H) Transient running speed reduction induced by indirect pathway stimulation also did not show difference between contralateral and ipsilateral blocks. Thus dMSN activation in our experiments did not increase the vigor of running.

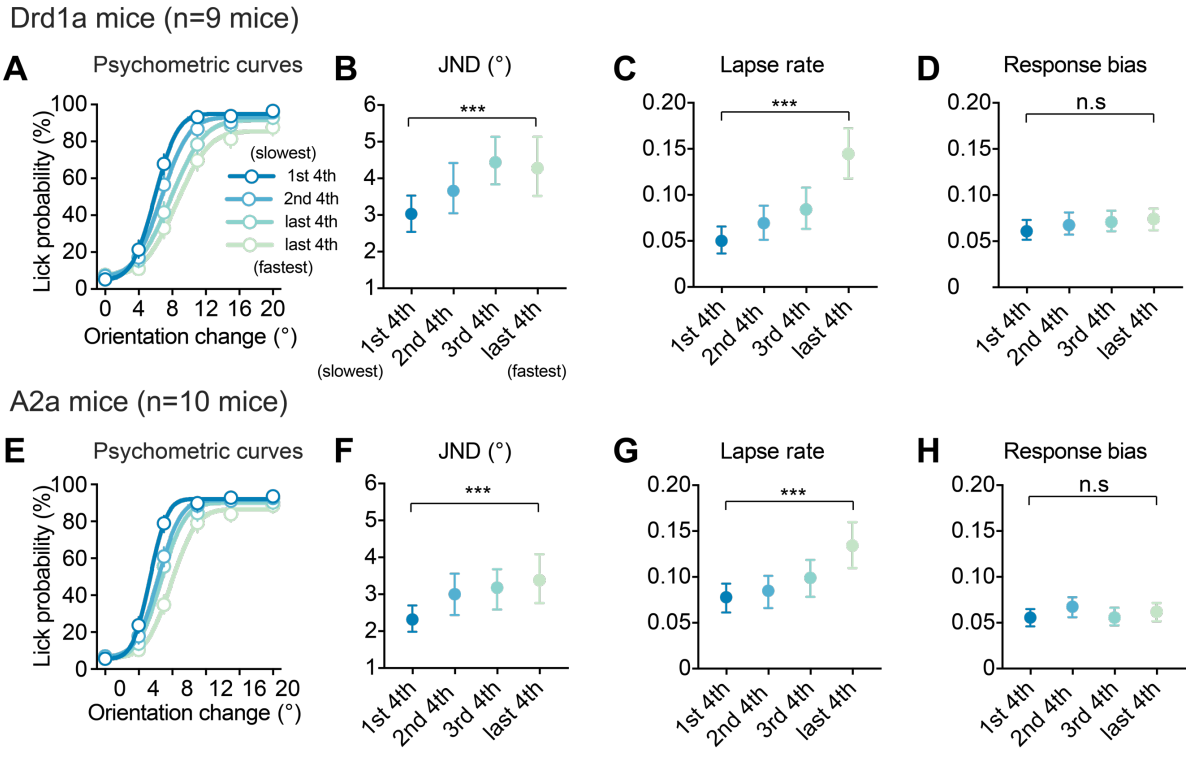

Figure S4: Impact of running speed on detection performance (related to Figure 5)

(A) Population psychometric curves of Drd1a mice without optogenetic stimulation. We divided the trials from each mouse into quartiles based on the running speed in the 500-ms interval preceding the change epoch, and pooled data from all the mice from the same genotype together to generate population psychometric curves separately for each quartile. (B) Effect of running speed on JND of Drd1a mice ($p<0.001$, One-way ANOVA of bootstrapped samples). Trials with fastest speed had significantly larger JND than slowest trials ($p<0.001$, non-parametric Wilcoxon test). (C) Effect of running speed on lapse rate ($p<0.001$). Trials with fastest speed had significantly larger lapse than slowest trials ($p<0.001$). D) Running speed did not change response bias ($p=0.16$). (E) Population psychometric curves of A2a mice divided into quartiles based on running speed. (F-G) Running also significantly influenced JND (F) and lapse rate (G) in A2a mice ($p<0.001$), faster trials had higher JNDs and lapse rates. H) No significant effect of running speed on response bias in A2a mice ($p=0.24$). Error bars indicate 95% confidence intervals.

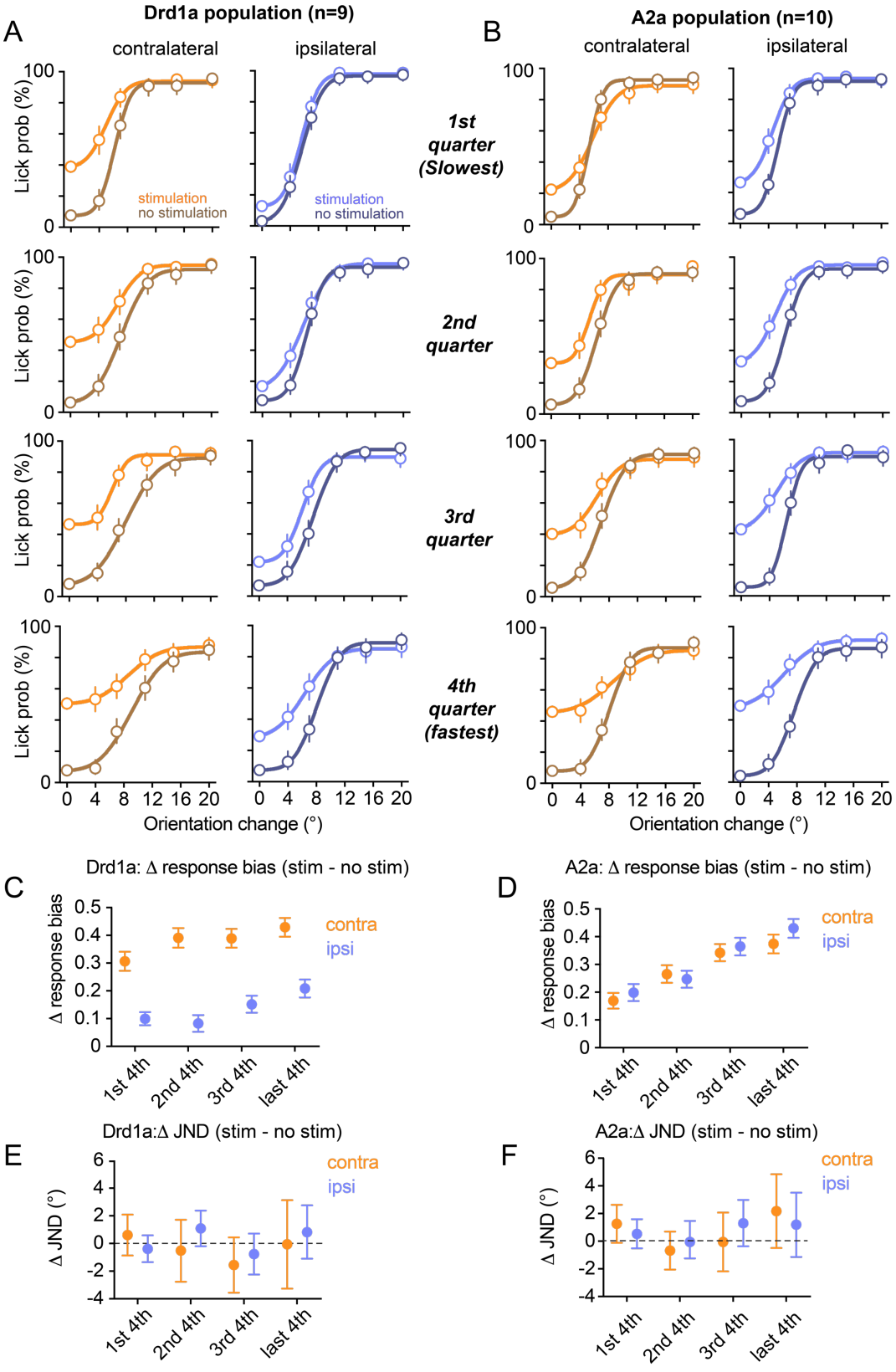
A
Drd1a population (n=9)
contralateral
ipsilateral
Lick prob (%)
stimulation
no stimulation
1st quarter (Slowest)
2nd quarter
3rd quarter
4th quarter (fastest)
Orientation change (°)
B
A2a population (n=10)
C
Drd1a: Δ response bias (stim - no stim)
Δ response bias
contra
ipsi
1st 4th
2nd 4th
3rd 4th
last 4th
D
A2a: Δ response bias (stim - no stim)
E
Drd1a:Δ JND (stim - no stim)
Δ JND (°)
F
A2a:Δ JND (stim - no stim)

Figure S5: Impact of running speed on changes in detection performance with optogenetic stimulation (related to Figure 5)

(A) Population psychometric curves of Drd1a mice with and without optogenetic stimulation sorted by running speed quartiles. (B) Population psychometric curves of A2a mice with and without optogenetic stimulation sorted by running speed quartiles. (C) Amplitude of direct pathway stimulation induced response bias shift (stimulation minus no stimulation) in running speed quartiles. ΔResponse bias on the contralateral side was significantly ($p<0.001$, non-parametric Wilcoxon test) higher than ipsilateral side in all 4 quartiles. (D) Amplitude of indirect pathway stimulation induced response bias shift in running speed quartiles. None of the quartiles showed significant ($P>0.05$) spatial bias between the two sides. (E-F) Neither direct nor indirect pathway stimulation significantly changed JND regardless of running speed (Drd1a: $p=0.27$, one-way ANOVA; A2a: $p=0.13$). Thus, striatal stimulation altered detection performance by changing response bias but not sensitivity, regardless of running speed. Error bars indicate 95% confidence intervals.

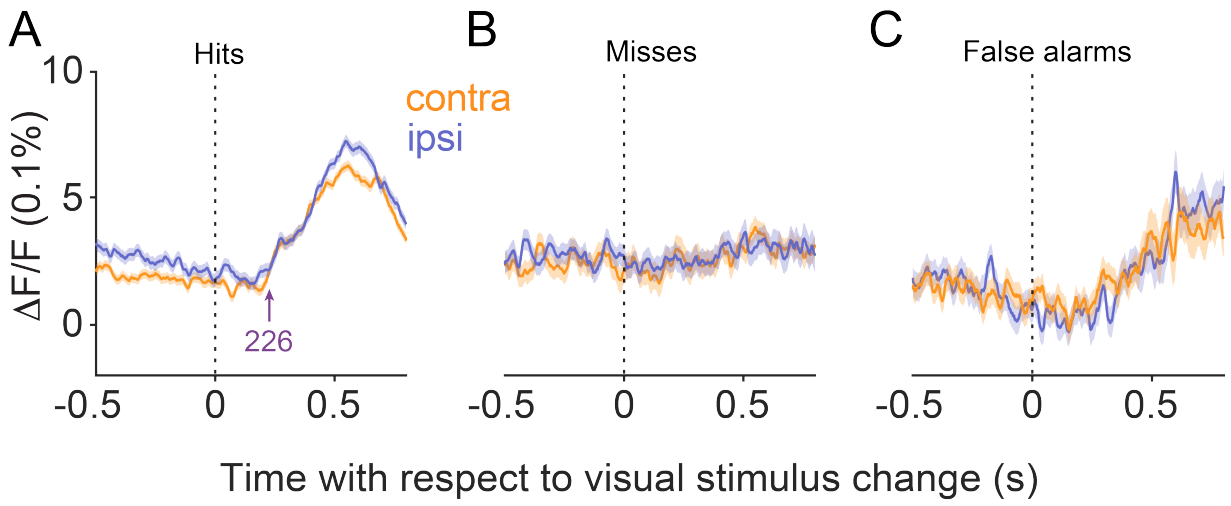

Figure S6: Timing of GCaMP activity with respect to visual stimulus change (related to Figure 8)

(A) Time course of population mean ΔF/F GCaMP traces aligned on change onset in trials with hits when the orientation change occurred in the contralateral (orange) or ipsilateral (blue) visual hemifield. Thick lines represent population mean and shading indicates SEM. Vertical purple arrow indicates mean onset timing (226-ms) of GCaMP transient. (B) Population GCaMP traces aligned on change onset in miss trials; no significant GCaMP transients were observed. (C) Population GCaMP activities aligned to change-epoch onset in false alarm trials. These results suggest that the GCaMP signals of dMSNs measured in our task were not due to visual events, but related to the decision to lick.